

# Development of Double-Stranded siRNA Labeling Method Using Positron Emitter and Its In Vivo Trafficking Analyzed by Positron Emission Tomography

Kentaro Hatanaka,<sup>†</sup> Tomohiro Asai,<sup>†</sup> Hiroyuki Koide,<sup>†</sup> Eriya Kenjo,<sup>†</sup> Takuma Tsuzuku,<sup>†</sup> Norihiro Harada,<sup>‡</sup> Hideo Tsukada,<sup>‡</sup> and Naoto Oku<sup>\*,†</sup>

Department of Medical Biochemistry and Global COE Program, Graduate School of Pharmaceutical Sciences, University of Shizuoka, 52-1 Yada, Suruga-ku, Shizuoka-city, Shizuoka 422-8526, Japan, and PET Center, Central Research Laboratory, Hamamatsu Photonics K.K., 5000 Hirakuchi, Hamakita-ku, Hamamatsu-city, Shizuoka 434-8601, Japan. Received December 7, 2009; Revised Manuscript Received February 8, 2010

Pharmacokinetic study of small interfering RNA (siRNA) is an important issue for the development of siRNAs for use as a medicine. For this purpose, a novel and favorable positron emitter-labeled siRNA was prepared by amino group-modification using *N*-succinimidyl 4-[fluorine-18] fluorobenzoate ([<sup>18</sup>F]SFB), and real-time analysis of siRNA trafficking was performed by using positron emission tomography (PET). Naked [<sup>18</sup>F]-labeled siRNA or cationic liposome/[<sup>18</sup>F]-labeled siRNA complexes were administered to mice, and differential biodistribution of the label was imaged by PET. The former was cleared quite rapidly from the bloodstream and excreted from the kidneys; but in contrast, the latter tended to accumulate in the lungs. We also confirmed the biodistribution of fluorescence-labeled naked siRNA and cationic liposome/siRNA complexes by use of a near-infrared fluorescence imaging system. As a result, a similar biodistribution was observed, although quantitative data were obtained only by planar positron imaging system (PPIS) analysis but not by fluorescence in vivo imaging. Our results indicate that PET imaging of siRNA provides important information for the development of siRNA medicines.

## INTRODUCTION

Small interfering RNA (siRNA) is a short double-stranded nucleic acid molecule that induces sequence-dependent gene silencing (1, 2), and gene therapy using siRNA is expected to be a novel treatment strategy for various diseases (3). However, the degradation of naked siRNA after administration into the bloodstream of human and animals readily occurs due to nucleases in the blood. Furthermore, siRNA poorly penetrates the plasma membranes of target cells, thus making difficult the delivery to the cytosol of targeted cells for effective gene knockdown. Therefore, a delivery system of siRNA molecules is considered to be indispensable for establishing siRNA therapy. Many studies on the in vivo application of siRNA using chemical modification (4) or drug delivery system (DDS) carriers such as liposomes (5) and micelles (6) for efficacious delivery and gene silencing have been reported. Cationic liposomes or micelles are representative carriers having electric charges on their surface. Because siRNA possesses polyanionic charges, it electrostatically interacts with cationic carriers used for RNA interference (RNAi). Pharmacokinetic studies on siRNA/carrier complexes have been performed by using fluorescence- or radioisotope-labeled carriers or carrier-entrapped imaging agents for magnetic resonance imaging. The techniques of carrier-labeling, however, do not always reflect the biodistribution of siRNA, since there is a chance that the siRNA may become detached from the carrier in the bloodstream, especially when the siRNA is bound to the surface of cationic carriers.

To evaluate the in vivo behavior of siRNA itself, the trafficking of it is carried out by near-infrared fluorescence (NIRF) imaging (7). However, like fluorescence imaging, NIRF imaging is affected by tissue depth to some extent, and therefore, quantitative data are difficult to obtain. In addition, although the NIRF imaging method is applicable for use on nonhuman primates, the method for human use has not yet been established.

To obtain precise pharmacokinetic information on siRNA molecules or their carriers in vivo, positron emission tomography (PET) is one of the ideal techniques. PET enables the determination of the real-time biodistribution and topical accumulation of positron emitter-labeled compound noninvasively. This technique can be applied in preclinical studies, in which a drug candidate labeled with a positron emitter is injected into animals. The circulation profile, biodistribution in various tissues, and eventual elimination of the drug candidate from the body can be monitored noninvasively in the same animal. Furthermore, certain positron emitter-labeled new drug candidates can be used for microdosing studies in humans. Such phase zero studies enable the investigator to reduce the rate of dropout of drug candidates in further clinical studies. For the pharmacokinetic study of DDS carriers, we previously reported a novel [<sup>18</sup>F]-probe for labeling the lipid assembly carriers for PET analysis (8). As mentioned above, since siRNA may possibly dissociate from its carrier and be degraded by plasma nucleases after injection into the bloodstream, we have sought to label siRNA with a positron emitter for the analysis of siRNA trafficking in vivo. The pharmacokinetic information on siRNA molecules, like that of the carrier, is considered to be critical and indispensable for the development of siRNA medicines.

Recently, Bartlett et al. labeled the sense strand of siRNA with copper-64 by using 1,4,7,10-tetraazacyclododecane-*N,N',N'',N'''*-tetraacetic acid (DOTA) and then annealed this modified strand with the unmodified antisense strand for the determining biodistribution of siRNA in micellar carriers (9).

\* Corresponding author. Naoto Oku, Department of Medical Biochemistry, University of Shizuoka School of Pharmaceutical Sciences, 52-1 Yada, Suruga-ku, Shizuoka 422-8526, Telephone number: +81-54-264-5701, Fax number: +81-54-264-5705, E-mail address: oku@u-shizuoka-ken.ac.jp.

<sup>†</sup> University of Shizuoka.

<sup>‡</sup> Hamamatsu Photonics K.K.

Viel et al. reported the conjugation of  $^{18}\text{F}$  to oligonucleotide by using (*N*-[3-(2- $^{18}\text{F}$ fluoropyridin-3-yloxy)-propyl]-2-bromoacetamide ( $^{18}\text{F}$ FRyBrA), and this method also required the annealing process (10, 11). In spite of their efforts, detail pharmacokinetic information about naked siRNA or siRNA in DDS carriers is still largely lacking.

In the present study, we developed a novel technique for labeling siRNA with a positron emitter,  $^{18}\text{F}$ , in which double-stranded siRNA was labeled to gain conformational accuracy for examining the pharmacokinetics of siRNA by using [ $^{18}\text{F}$ ]SFB as an  $^{18}\text{F}$  labeling reagent. [ $^{18}\text{F}$ ]SFB have been widely used to form a stable amide bond by reacting with primary amino groups for a short time and very easily for labeling certain peptides (12), antibodies (13), or DNA oligonucleotides (14). Because  $^{18}\text{F}$  has an extremely short half-life (109 min), avoidance of the annealing process by labeling of double-stranded siRNA is favorable. [ $^{18}\text{F}$ ]-labeled siRNA thus prepared was identified by ESI-TOF-MS, HPLC, and autoradiography after electrophoresis. By use of this positron emitter-labeled siRNA, we actually examined the biodistribution of siRNA by PPIS in the presence or absence of cationic liposome, a DDS carrier of siRNA. We also performed NIRF imaging for verifying the in vivo behavior of siRNA and discussed the correspondence of the imaging results obtained from NIRF imaging and PPIS imaging.

## EXPERIMENTAL PROCEDURES

**Materials.** 4,7,13,16,21,24-Hexaoxa-1,10-diazabicyclo[8.8.8]-hexacosane (K[2.2.2]), tetra-*n*-propyl-ammonium hydroxide ( $\text{Pr}_4\text{NOH}$ ), *N,N,N',N'*-tetramethyl-*O*-(*N*-succinimidyl)uronium tetrafluoroborate (TSTU),  $\text{CH}_3\text{CN}$  (anhydrous), and fetal bovine serum were obtained from Sigma-Aldrich (Saint Louis, MO, USA). Potassium carbonate  $\cdot 1.5\text{H}_2\text{O}$  was purchased from Merck (Darmstadt, Germany). Anion-exchange resin AG1-X8 ( $\text{OH}^-$  form, 100–200 mesh) was from Bio-Rad Laboratories (Hercules, USA). *N,N*-Dimethylformamide (DMF) was purchased from Wako Pure Chemical Industries, Ltd. (Osaka, Japan). A cationic lipid for transgene use, 1,2-dioleoyl-3-trimethylammonium-propane (DOTAP), was purchased from Avanti Polar Lipids Inc. (Alabaster, AL, USA). Cholesterol was kindly provided by Nippon Fine Chemical Co., Ltd. (Takasago, Hyogo, Japan). Trizol reagent was obtained from Invitrogen Co. (Carlsbad, CA). An alfalfa-free feed was purchased from Oriental Yeast co. Ltd. (Tokyo, Japan). Escain was purchased from Mylan Pharmaceuticals (Morgantown, WV). All other chemicals and solvents were analytical grade and were used without further purification unless otherwise stated. [ $^{18}\text{F}$ ]Fluoride was produced with a cyclotron (HM-18, Sumitomo Heavy Industries, Tokyo, Japan) at Hamamatsu Photonics PET Center by the  $^{18}\text{O}(\text{p},\text{n})^{18}\text{F}$  nuclear reaction using [ $^{18}\text{O}$ ]H $_2\text{O}$ . Labeled compounds were synthesized by using modified CUPID system (Sumitomo Heavy Industries, Tokyo, Japan). The HPLC column used for the purification of succinimidyl 4- $^{18}\text{F}$  fluorobenzoate ([ $^{18}\text{F}$ ]SFB) was an Inertsil ODS3 (10  $\times$  250 mm, 5  $\mu\text{m}$ , GL Sciences Inc., Tokyo, JAPAN). Nonradioactive fluorine-conjugated siRNA was identified by using a UPLC/ESI-QTOF-MS system, which consisted of an ACQUITY ultraperformance liquid chromatography (UPLC) system and an electrospray ionization quadrupole time-of-flight mass spectrometer (SYNAPT High Definition Mass Spectrometry system; Waters, Milford, MA, USA). An ultraviolet–visible (UV/vis) detector (ACQUITY TUV, Waters) was used. The UPLC column used for the identification of fluorine-labeled siRNA was an Acquity UPLC BEH C18 column (2.1  $\times$  100 mm, 1.7  $\mu\text{m}$ , Waters Corp.). The particle size and zeta-potential of nanoparticles were measured by using a Zetasizer Nano ZS (Malvern, Worcs, UK). Gel for obtaining an autoradiogram of  $^{18}\text{F}$  and siRNA after electrophoresis was used an FLA-7000 (FUJIFILM Corporation, Tokyo, Japan) and LAS-3000 mini

system (Fuji Film, Tokyo, Japan), respectively. Fluorescence imaging was performed by using a Xenogen IVIS Lumina System coupled to *Living Image* software for data acquisition (Xenogen Corp., Alameda, CA). PET imaging was performed by using a planar positron imaging system (PPIS, Hamamatsu Photonics, Shizuoka, Japan). Radioactivities in each organs were measured by gamma-counter (ARC-2000, Aloka, Tokyo, Japan).

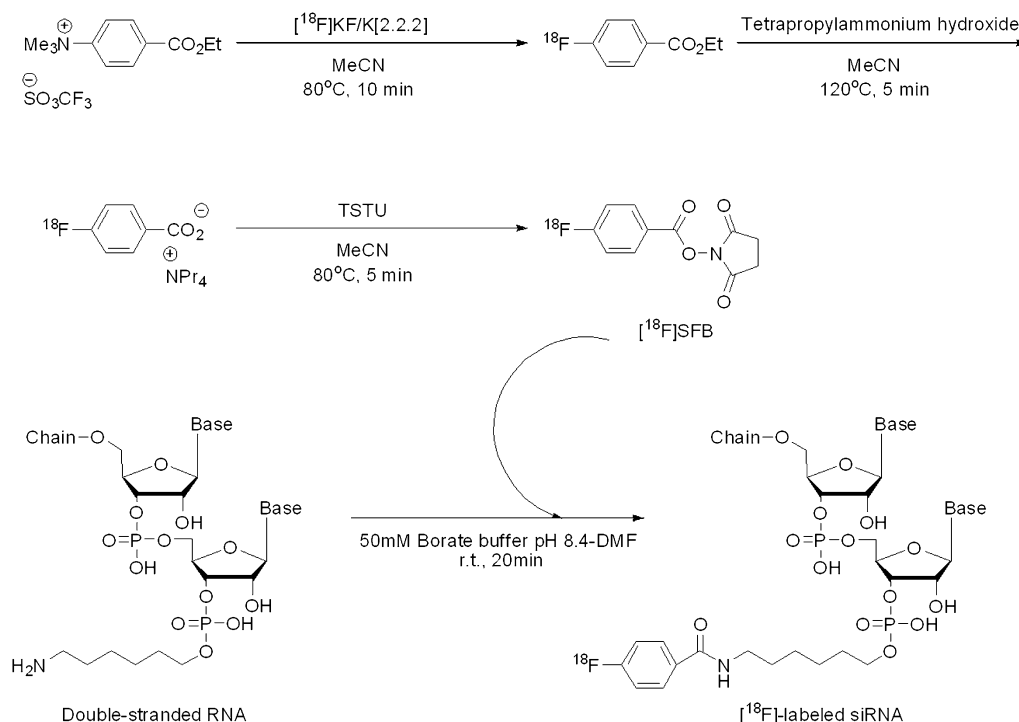
**Experimental Animals.** Five-week-old male BALB/c mice male were purchased from Japan SLC Inc. (Shizuoka, Japan). The animals were cared for according to the Animal Facility Guidelines of the University of Shizuoka. All animal experiments were approved by the Animal and Ethics Review Committee of the University of Shizuoka.

**siRNA Sequence.** Alexa Fluor 750-labeled siRNA (AF750-siRNA) was purchased from Japan Bio Services Co., Ltd. (Saitama, Japan). Antisense strand contained a fluorescence at the 3' end of the strand. siRNA for positron emitter-labeling was synthesized and purified by Hokkaido System Science. The nucleotide sequences of the siRNA were those of an unspecific scrambled RNA, and the antisense strand contained a 3' amino C6 linker for the radioactive labeling of the siRNA duplex (Scheme 1). The sequences of the siRNA used were 5'-CGAUUCGCUAGACCGGCUUCAUUGCAG-3' (sense) and 5'-GCAUGAAGCCGGUCUAGCGAAUCGAU-3' (antisense).

**Synthesis of Ethyl-(4-Trimethylammonium)benzoate Tri-fluoromethanesulfonate.** Ethyl 4-dimethylaminobenzoate was synthesized according to the procedure reported by Haka et al. (15). The synthetic compound was assigned by  $^1\text{H}$  NMR and  $^{13}\text{C}$  NMR. Ethyl 4-dimethylaminobenzoate 11.4 g (59 mmol) was dissolved in 70 mL anhydrous  $\text{CH}_2\text{Cl}_2$ . Ten grams of  $\text{CF}_3\text{SO}_3\text{CH}_3$  (64.9 mmol) was added dropwise to the solution, and the mixture was stirred overnight at room temperature. A crystalline precipitate was formed by the addition of  $\text{Et}_2\text{O}$  (100 mL) and collected by suction filtration. Recrystallization from  $\text{CH}_2\text{Cl}_2/\text{Et}_2\text{O}$  gave 10.2 g (48%) of ethyl 4-trimethylammoniumbenzoate trifluoromethanesulfonate.

**Radiosynthesis of [ $^{18}\text{F}$ ]KF/K[2,2,2] Complex.** [ $^{18}\text{F}$ ]KF/K[2,2,2] was obtained by use of a previously reported method (16). In brief, [ $^{18}\text{F}$ ]fluoride was trapped by ion-exchange resin AG1-X8 and eluted from the resin by 0.5 mL of 40 mM  $\text{K}_2\text{CO}_3$ . To this fluoride solution, 15 mg of K[2,2,2] in  $\text{CH}_3\text{CN}$  (2 mL) was added. Water was removed by azeotropic distillation at 110  $^\circ\text{C}$  under He flow (400 mL/min) for 5 min. To the residue, the addition of  $\text{CH}_3\text{CN}$  (1 mL) and azeotropic distillation were repeated twice. Then, the residue was dried under reduced pressure for 1 min, and the reaction vessel was purged with a flow of He (50 mL/min) for 1 min to ensure complete dryness. Finally, the reaction vessel was cooled to room temperature and used for further labeling.

**Preparation of Succinimidyl 4- $^{18}\text{F}$  fluorobenzoate ([ $^{18}\text{F}$ ]SFB).** [ $^{18}\text{F}$ ]SFB was prepared according to the one-pot procedure of Tang et al. (17) with some modifications. The precursor (5 mg) in 1.5 mL of  $\text{CH}_3\text{CN}$  was added to the dried [ $^{18}\text{F}$ ]KF/K[2,2,2] complex mentioned above and reacted at 80  $^\circ\text{C}$  for 10 min. After the reaction mixture had been cooled, 20  $\mu\text{L}$  of 1 M  $\text{Pr}_4\text{NOH}$  in 0.5 mL of  $\text{CH}_3\text{CN}$  was added; and hydrolysis was carried out at 120  $^\circ\text{C}$  for 5 min. Then, to the reaction mixture, TSTU (15 mg) in 0.5 mL of  $\text{CH}_3\text{CN}$  was added and converted to [ $^{18}\text{F}$ ]SFB at 80  $^\circ\text{C}$  for 5 min. The reaction mixture was diluted with 2.0 mL of 5%  $\text{CH}_3\text{COOH}$  and transferred to the HPLC injector. Crude product was purified by semipreparative HPLC ( $\text{CH}_3\text{CN}:\text{H}_2\text{O} = 300:700$ , 6 mL/min, 254 nm). The radioactive peak eluted at 25.7 min was collected, diluted with 30 mL of  $\text{H}_2\text{O}$ , and passed through a Sep-Pak C18 cartridge (Waters). [ $^{18}\text{F}$ ]SFB retained on the cartridge was released with 4 mL of  $\text{CH}_2\text{Cl}_2$  and recovered into a V-vial by passage through a Sep-Pak Dry cartridge (Waters). Then, the [ $^{18}\text{F}$ ]SFB was concen-

**Scheme 1. Synthesis of the [ $^{18}\text{F}$ ]SFB and [ $^{18}\text{F}$ ]-Labeled siRNA****Table 1. Gradient Flow Table**

time (min)	0.1 M TEAA (%)	CH <sub>3</sub> CN (%)	flow rate (mL/min)
0–2	95–90	5–10	0.3
2–3	90–75	10–25	0.3
3–7	75–60	25–40	0.3
7–10	60–0	40–100	0.3

trated by a flow of He (200 mL/min) at 60 °C and used for labeling. [ $^{18}\text{F}$ ]SFB with (a specific radioactivity of 51.4 GBq/ $\mu\text{mol}$ , a radiochemical yield of 21.1%) was obtained.

**Radiolabeling of siRNA with [ $^{18}\text{F}$ ]SFB.** siRNA (40 nmol) in 16  $\mu\text{L}$  of 50 mM borate buffer, pH 8.5, was added to the [ $^{18}\text{F}$ ]SFB (60 nmol) in 3.6  $\mu\text{L}$  of DMF. The mixture was vortexed for a few seconds and then incubated at room temperature for 20 min. The reaction mixture was purified and concentrated by ultrafiltration through a 10 000 molecular weight cutoff filter (Amicon, Millipore, Bedford, MA, USA). The mixture was centrifuged at  $4000 \times g$  with RNase-free phosphate-buffered saline (PBS). [ $^{18}\text{F}$ ]-labeled siRNA with a radiochemical yield of 37.9% and a specific activity of 25.5 GBq/ $\mu\text{mol}$  was obtained. Nonradioactive fluorine-conjugated siRNA was synthesized in a similar manner except that 150 nmol cold SFB was used instead of 60 nmol [ $^{18}\text{F}$ ]SFB.

**Analytical Methods.** Nonradioactive fluorine-conjugated siRNA was identified by using a UPLC/ESI-QTOF-MS system. The analytical column was maintained at 40 °C. A ultraviolet–visible (UV/vis) detector, equipped with a 500 nL flow cell, was also directly connected between the column outlet and the QTOF-MS instrument. Fractionation of fluorine-conjugated siRNA was performed at a flow rate of 0.3 mL/min using as the eluent the gradient of 0.1 M triethylammonium acetate (TEAA, pH 7.0) and CH<sub>3</sub>CN. Gradient profile is presented in Table 1.

**Evaluation of siRNA Labeling.** Precursor siRNA, fluorine-conjugated siRNA (non-RI), and [ $^{18}\text{F}$ ]-labeled siRNA (0.5  $\mu\text{g}$ ) were applied to a 15% polyacrylamide gel and electrophoresed. Then, the gel was exposed to an imaging plate for obtaining an autoradiogram of  $^{18}\text{F}$  by using an FLA-7000; the gel was stained for 5 min in ethidium bromide (EtBr), and siRNA was detected by using a LAS-3000 mini system.

**Preparation of Cationic Liposomes and Their Complexes with siRNA.** DOTAP and cholesterol (1:1 as a molar ratio) were dissolved in *tert*-butyl alcohol for freeze–drying and hydrated in RNase-free PBS. The liposomes were frozen and thawed for 3 cycles using liquid nitrogen and extruded 10 times through a polycarbonate membrane filter having a pore size of 100 nm (Nucleopore, Maidstone, UK). Then, the cationic liposome and siRNA were mixed gently and incubated for 10 min at room temperature to form liposome/siRNA complexes. The nitrogen moiety of cationic liposome to the phosphorus of siRNA (N/P ratio) was 24:1 in the complexes. The particle size and zeta-potential of liposome/siRNA complexes diluted with RNase-free PBS were measured. The particle size of liposome/siRNA complexes was  $218 \pm 3.0$  nm ( $n = 3$ ), and the particles showed monodispersion (polydispersity index = 0.16). The zeta-potential was  $36.3 \pm 1.9$  mV.

**Near-Infrared Fluorescence Imaging in Vivo.** The biodistribution of AF750-siRNA was assessed by using an IVIS Lumina System. Mice were fed an alfalfa-free feed to reduce the effect of background fluorescence. The animals were anesthetized continuously via inhalation of 2% escain. siRNA or liposome/siRNA complexes containing 15  $\mu\text{g}$  AF750-siRNA were injected via a tail vein under anesthesia. Alexa Fluor 750 fluorescence was acquired every 10 min for up to 60 min after the injection. After monitoring, the mice were sacrificed under anesthesia. Then, the organs, namely, heart, lungs, liver, spleen, and kidneys, were collected and imaged *ex vivo* with the IVIS.

**PPIS Imaging of [ $^{18}\text{F}$ ]-Labeled siRNA.** Biodistribution of [ $^{18}\text{F}$ ]-labeled siRNA was imaged noninvasively by using a PPIS (18–20). Animals were anesthetized with an intraperitoneal injection of pentobarbital at 50 mg/kg, and then fixed on an animal holder. To determine the whole-body biodistribution of siRNA, we administered the [ $^{18}\text{F}$ ]-labeled siRNA intravenously (2.5 MBq/mouse). The scan was started immediately after the administration and performed for 60 min. Images were analyzed by using software *ImageJ*. After the PPIS scan, the mice were sacrificed for the collection of the blood from a carotid artery under anesthesia. Then, the heart, lungs, liver, spleen, and kidneys were removed, and the biodistribution of



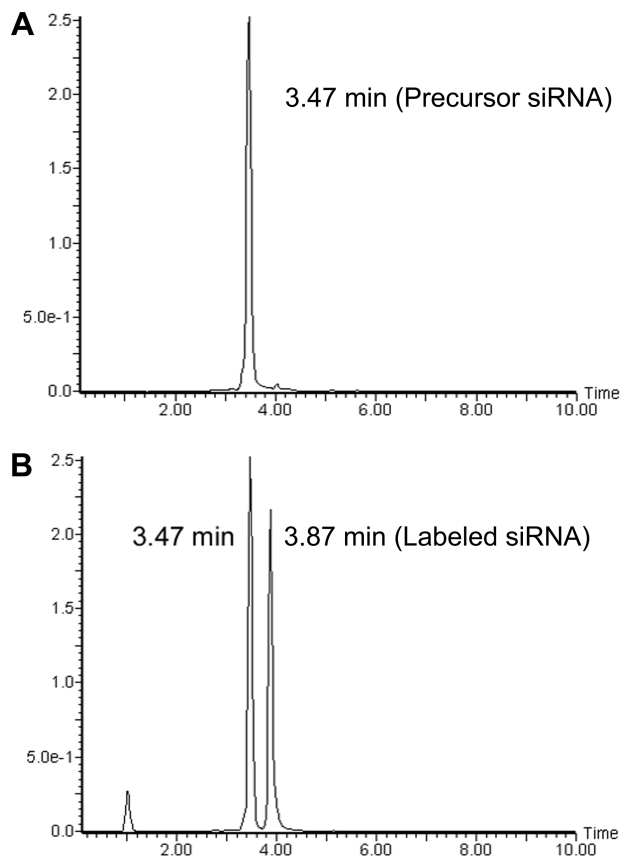


**Figure 1.** UPLC analysis of fluorine-conjugated siRNA. Nonradioactive fluorine was conjugated to siRNA and separated with the UPLC system. (A) Peak of precursor siRNA at 3.47 min. (B) Peaks of unreacted siRNA at 3.47 min and fluorine-labeled siRNA at 3.87 min after the reaction.

[ $^{18}\text{F}$ ]-labeled siRNA was measured with a gamma counter. Distribution data were presented as percent dose per wet tissue. The total volume of blood was assumed to be 7.56% of the body weight. A time–activity curve was obtained from the mean pixel radioactivity in the region of interest (ROI) of the PPIS images.

**Evaluation of siRNA Stability against Serum-Mediated Degradation.** Fluorine-conjugated (0.5  $\mu\text{g}$ ) naked siRNA or that complexed with liposomes was incubated in 90% fetal bovine serum for 60 min at 37  $^{\circ}\text{C}$ . The siRNA was extracted from the serum by using Trizol reagent and subjected to 15% polyacrylamide gel electrophoresis. The gel was stained for 5 min in EtBr, and siRNA was detected by using a LAS-3000 mini system.

## RESULTS

**[ $^{18}\text{F}$ ]-Labeling of siRNA and Its Radiochemistry.** The methods for synthesis of [ $^{18}\text{F}$ ]SFB and [ $^{18}\text{F}$ ]-labeling of siRNA are shown in Scheme 1. At first, we prepared non-radioisotope (non-RI) fluorine-conjugated siRNA and identified the compound by using LC/ESI-TOF-MS (Table 1). Unreacted siRNA showed a peak at 3.47 min (Figure 1A). After the reaction, HPLC analysis indicated 2 main peaks, namely, labeled siRNA at 3.87 min and precursor siRNA at 3.47 min, respectively (Figure 1B). These peaks were fractionated by HPLC and analyzed by ESI-TOF-MS, giving multiply charged ion peaks of  $m/z$  [M-8H] $^{8-}$  2196.1, [M-7H] $^{7-}$  2510.9, and [M-6H] $^{6-}$  2930.0 (data not shown), which corresponded to the labeled siRNA (expected mass of  $m/z$  [M-8H] $^{8-}$  2196.7, [M-7H] $^{7-}$  2510.7, and [M-6H] $^{6-}$  2929.3). The overall yield of labeled siRNA was greater than 30% based on the peak area. On the

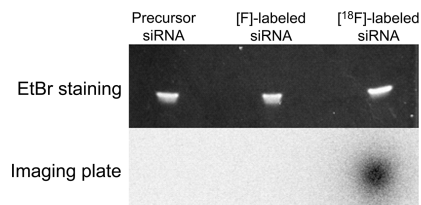


**Figure 2.** Demonstration of [ $^{18}\text{F}$ ] labeling of siRNA. Precursor siRNA, fluorine-conjugated siRNA, and [ $^{18}\text{F}$ ]-labeled siRNA were applied to a 15% polyacrylamide gel, electrophoresed, and stained with ethidium bromide. The gel was exposed to an imaging plate for detecting  $^{18}\text{F}$ .

basis of the result from non-RI fluorine-grafting to siRNA, [ $^{18}\text{F}$ ]-labeled siRNA was prepared according to the same procedure, and then electrophoresis assay and subsequent autoradiography were performed to confirm the production of [ $^{18}\text{F}$ ]-labeled siRNA. Electrophoresis assay with an imaging plate showed that the siRNA was labeled with [ $^{18}\text{F}$ ]-fluorine without any other exposure bands (Figure 2). In addition, the main band visualized by EtBr staining showed the same position as the band on the same polyacrylamide gel observed by autoradiography. As a result, [ $^{18}\text{F}$ ]-labeled siRNA was successfully prepared without any positron emitter-labeled byproducts, and the labeled siRNA was not degraded under the experimental conditions used.

**Biodistribution of siRNA Determined with near-Infrared Fluorescence Imaging in Vivo.** We examined the in vivo behavior of siRNA by use of the NIRF imaging system. Mice were intravenously administered naked AF750-siRNA or liposome/AF750-siRNA complexes via a tail vein. The fluorescence imaging of AF750-siRNA was started immediately after the injection and monitored for 60 min. The biodistribution of AF750-siRNA is shown in Figure 3. The results indicated that the fluorescence compound was accumulated in the bladder immediately after the administration of naked AF750-siRNA and then excreted in the urine (Figure 3A). On the contrary, fluorescence was observed at the upper part of the body where the lung was positioned after the administration of liposome/AF750-siRNA complexes. The total fluorescence intensity of the image of mice injected with naked AF750-siRNA was apparently higher than that obtained with the liposomal formulation: Fluorescence in bladder after injection of naked siRNA was quite intense because bladder is located near the body surface, while that in lungs after injection of cationic liposome complexes was weak because lungs are located more deep from body surface compared with bladder.

The ex vivo imaging showed that a small amount of fluorescence remained in the kidneys but that no fluorescence was detected in the other tissues examined (Figure 3B). In contrast, the fluorescence of the cationic liposome/AF750-siRNA complexes accumulated in the lungs, being consistent with the in vivo imaging data.

**Stability of Fluorine-Conjugated siRNA against Serum-Mediated Degradation.** We evaluated the stability of naked fluorine-conjugated siRNA and cationic liposome/fluorine-conjugated siRNA complexes in serum for 60 min (Figure 4). The naked fluorine-conjugated siRNA incubated in PBS (control) was not decomposed. However, the band of naked siRNA obtained by electrophoresis of the sample that had been incubated in the presence of serum disappeared, indicating that the siRNA had been degraded by RNase within 60 min. In contrast, the band of siRNA was detected in the case of the cationic liposome/siRNA complexes exposed to the serum, indicating that complex formation protected siRNA from RNase in the serum.

**In Vivo PPIS Imaging of siRNA Trafficking.** Next, we examined [ $^{18}\text{F}$ ]-labeled siRNA trafficking by use of PPIS. Mice were intravenously administered naked [ $^{18}\text{F}$ ]-labeled siRNA in

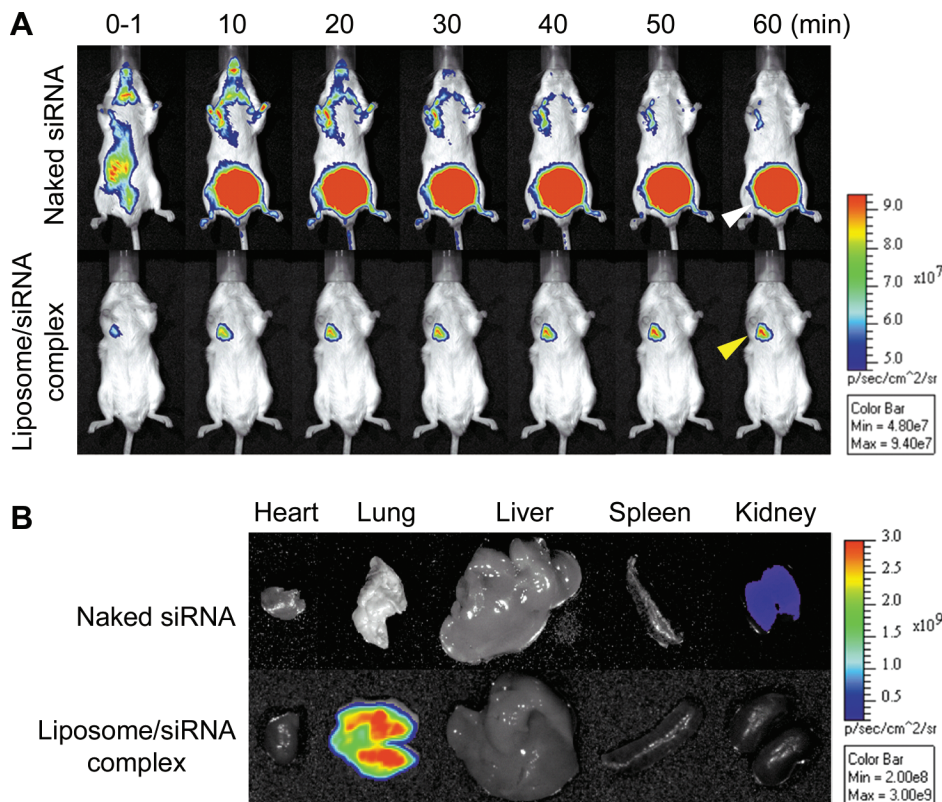


**Figure 3.** NIRF in vivo imaging with AF750-siRNA and liposome/AF750-siRNA complexes. (A) AF750-siRNA (top) or liposome/AF750-siRNA complexes (bottom) were intravenously administered to BALB/c mice. Images were acquired every 10 min for up to 60 min after the administration. The white arrowhead shows the bladder region, and the yellow arrowhead, the lung region. (B) Ex vivo imaging of AF750-siRNA and liposome/AF750-siRNA complexes at 60 min after administration.

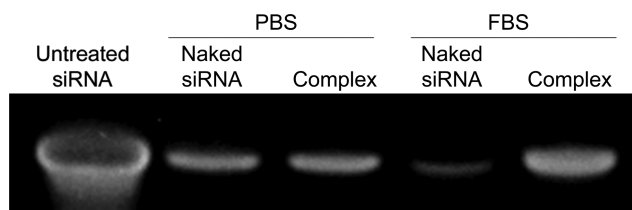


**Figure 4.** Stability of naked siRNA or liposome/siRNA complexes in FBS. siRNA (0.5  $\mu$ g) was incubated with PBS (–) or 90% FBS at 37 °C for 60 min. siRNA was extracted and electrophoresed on a 15% polyacrylamide gel after a 60 min incubation and stained with EtBr. Untreated siRNA was used as a control marker.

PBS (–) or liposome/ $^{18}\text{F}$ -labeled siRNA complexes via a tail vein. The real-time imaging of  $^{18}\text{F}$ -labeled siRNA using PPIS was acquired for 60 min, and images were integrated every 5 min (Figure 5A). The  $^{18}\text{F}$  radioactivity of the naked  $^{18}\text{F}$ -labeled siRNA accumulated inside the kidneys immediately after administration. This accumulation was not detected in NIRF in vivo imaging because of the influence of tissue depth. Then,  $^{18}\text{F}$  was transferred to the bladder and subsequently excreted in the urine. In contrast, most of the  $^{18}\text{F}$  radioactivity after the administration of cationic liposome/ $^{18}\text{F}$ -labeled siRNA complexes were retained in the lungs for 60 min, and only insignificant accumulation of them was observed in the bladder. The time–activity curve of  $^{18}\text{F}$  in naked siRNA showed transient accumulation in kidney immediately after injection (19% injected dose/tissue at 2 min), and half of that was transferred to bladder at 21 min, and then the excretion of  $^{18}\text{F}$  to bladder was gradually increased (Figure 5B). In contrast, the most of the  $^{18}\text{F}$  after injection of liposome/siRNA complexes immediately accumulated in lungs and was maintained up to 60 min (76% injected dose/tissue). The biodistribution data obtained with a gamma counter after organ dissection showed that the

$^{18}\text{F}$  after administration of naked  $^{18}\text{F}$ -labeled siRNA had not been distributed in any tissues tested, whereas the radioactivity after the injection of the cationic liposome/ $^{18}\text{F}$ -labeled siRNA complexes was highly distributed in the lungs (Figure 5C). These results corresponded roughly to the data obtained from the fluorescence ex vivo imaging.

Moreover, to confirm whether the accumulation of  $^{18}\text{F}$  in the lungs after administration of cationic liposome/ $^{18}\text{F}$ -labeled siRNA reflected the accumulation of the liposomes of the complex, we examined the biodistribution of cationic liposome/siRNA complexes prepared with  $^3\text{H}$ cholesterylhexadecyl ether as a component. As a result, the liposomal complexes with siRNA were distributed in the lungs quite similarly to the distribution of the  $^{18}\text{F}$ , suggesting that cationic liposome/siRNA accumulated in lungs as the complex form (Supporting Information Figure S1).

## DISCUSSION

Recently, the topical application of siRNA medicines has reached clinical trial, and siRNA delivery systems for systemic injection have been extensively studied for the next generation of siRNA medicines (21). Pharmacokinetic information on siRNA molecules is considered to be particularly important for the acceleration of the development of siRNA medicine. Among the technologies for pharmacokinetic analysis, PET imaging technique is considered to be applicable to both preclinical trial and microdosing study (human phase 0 study). Using subtoxic and subpharmacologic doses, PET microdosing studies can be performed to screen for drug candidates for clinical trials on the basis of their pharmacokinetic properties (22, 23).

In the present study, we labeled double-stranded siRNA with  $^{18}\text{F}$  to obtain pharmacokinetics information about siRNA and siRNA in DDS carriers. We used  $^{18}\text{F}$ -fluorine as a short-

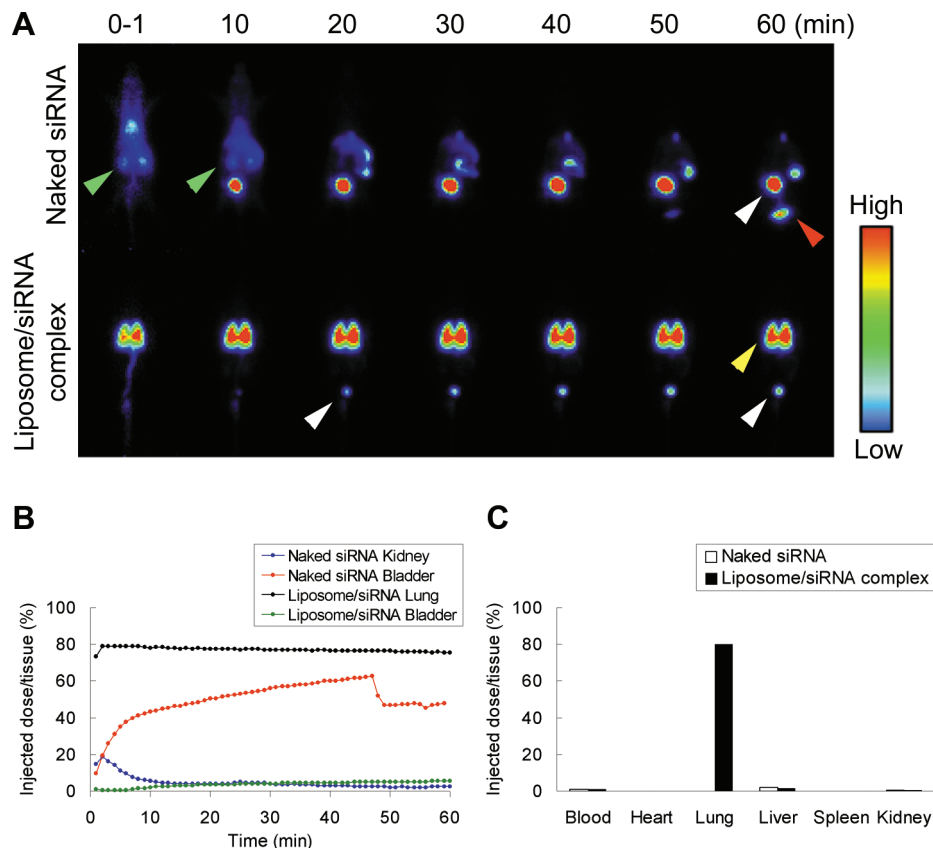


**Figure 5.** PPIS imaging with [ $^{18}\text{F}$ ]-labeled siRNA and liposome/ $^{18}\text{F}$ -labeled siRNA complexes. (A) Naked siRNA (top) or liposome/siRNA complexes (bottom) at 2.5 MBq in 0.2 mL were intravenously administered to BALB/c mice. Images were acquired with a 1 min frame at 1, 10, 20, 30, 40, 50, and 60 min after the administration. The green arrowhead shows kidneys; the white one, the bladder; the red one, urine; and the yellow one, the lungs. (B) Real-time changes in [ $^{18}\text{F}$ ]-labeled siRNA and liposomal [ $^{18}\text{F}$ ]-labeled siRNA. Time activity curves of  $^{18}\text{F}$  with naked siRNA shows kidney (blue) and bladder (red) and that of  $^{18}\text{F}$  with cationic liposome/siRNA shows lung (black) and bladder (green). (C) After the PPIS scan, the mice were sacrificed, and biodistribution of  $^{18}\text{F}$  in each organ was then measured with a gamma counter.

lived positron-emitting radionuclide (half-life: 109 min), which has been applied to humans for cancer diagnosis in the form of [2- $^{18}\text{F}$ ]2-deoxy-2-fluoroglucose ([ $^{18}\text{F}$ ]FDG). The advantages of the present methodology to label siRNA are that (1) the modification of double-stranded RNA with amino group enables fast preparation and purification without the time-consuming process of annealing and (2) the methodology maintains the conformational accuracy of the siRNA. Indeed, reaction of siRNA and [ $^{18}\text{F}$ ]SFB was complete within 20 min. In addition, fluorine-conjugated siRNA was identified by LC and ESI-TOF-MS (Figure 1) and did not decompose during the reaction or purification process (Figure 2).

It is well-known that one of the most important factors regarding the biodistribution of liposomes *in vivo* is the charge of the liposomal surface. Positively charged complexes aggregate in the presence of serum proteins (24), are entrapped in the lung capillaries, and thus accumulate in the lung tissue (25, 26) after intravenous administration. In fact, when liposomes were labeled with [ $^3\text{H}$ ]cholesterylhexadecyl ether, the radioactivity of cationic liposome/siRNA complexes accumulated in the lungs (Supporting Information Figure S1). However, since nucleic acids such as siRNAs and oligodeoxynucleotides (ODNs) are known to be eliminated from the circulation via the kidneys and excreted into the urine 60 min after administration via a tail vein (27, 28), distribution studies on siRNAs or ODNs besides on their carriers are important for the development of nucleic acid medicines. In the distribution study, [ $^3\text{H}$ ]cholesterylhexadecyl ether was accumulated in the liver to some extent, although the accumulation of siRNA was not observed after injection of cationic liposome/siRNA complex.

We speculate that siRNA was degraded in the liver and excreted, while cholesterylhexadecyl ether did not.

In the present study, we first used AF750-siRNA and examined its *in vivo* behavior by using NIRF fluorescence imaging. NIRF fluorescence was rapidly cleared from the bloodstream and excreted in the bladder after the administration of naked AF750-siRNA (Figure 3). In contrast, the fluorescence of cationic liposome/siRNA complexes accumulated in the lungs. However, the differential fluorescence intensities between *in vivo* images and *ex vivo* ones indicated the limitation of NIRF imaging. Quantitative analysis could not be applied due to the influence of tissue depth on the fluorescence intensity. Moreover, it is possible that fluorescence self-quenching and/or resonance energy transfer affect the intensity.

In contrast to NIRF imaging, PPIS or PET technology provides quantitative analytic data with high spatial resolution.  $^{18}\text{F}$  was observed in the kidneys until 10 min after the administration of naked [ $^{18}\text{F}$ ]-labeled siRNA, and subsequently, it was transferred to the bladder and excreted into urine (Figure 5). This result is consistent with previous result reported by Viel et al. who used  $^{18}\text{F}$ -labeled naked siRNA (17). Other reports also presented the renal excretion of siRNA (27, 29, 30). In addition, Bartlett et al. reported that the excretion of  $^{64}\text{Cu}$ -labeled naked siRNA was quite fast (9). They indicated that the siRNA in a complex with cyclodextrin-containing polycation excreted quite rapidly and suggested the instability of the complex. Therefore, determination of siRNA trafficking instead of carrier trafficking is important for the development of siRNA medicines. In contrast to the *in vivo* fate of naked siRNA, the  $^{18}\text{F}$  of



cationic liposome/[ $^{18}\text{F}$ ]-labeled siRNA complexes was spread throughout the lungs and was retained in them at least up to 60 min.

Next, we investigated the stability of siRNA in the presence of serum by performing an electrophoresis assay. The data indicated that naked siRNA was degraded when incubated for 60 min in serum, whereas the liposome/siRNA complexes were not (Figure 4). These results suggest that naked siRNA has a short half-life in vivo and is rapidly eliminated by renal excretion as a degraded form. However, further study is needed to clarify whether the excreted siRNA is in the intact form or degraded form. On the other hand, a part of the  $^{18}\text{F}$  showed enterohepatic circulation. This enterohepatic circulation would be mediated by some of the fragmented siRNA having the polar moiety (the alkyl chain on the 3' end of the antisense strand) and nonpolar moiety (siRNA).

As indicated above, the serum stability study showed that the liposomal siRNA was not degraded in the presence of serum. Furthermore, the  $^{18}\text{F}$  distribution of liposomal [ $^{18}\text{F}$ ]-labeled siRNA was similar to the distribution of the [ $^3\text{H}$ ]-labeled liposome carrier: Both were accumulated in the lungs after intravenous administration. Taken together, our data strongly suggest that liposomal siRNA would be delivered to the lungs in its intact form. In conclusion, we developed a novel positron emitter-labeling methodology for siRNA and evaluated the in vivo trafficking of [ $^{18}\text{F}$ ]-labeled siRNA by PPIS. The results of present study suggest that siRNA is stable as a complex with liposomes and should be deliverable specific tissues depending on the characteristics of the carrier. Therefore, designing the DDS carrier expands the usefulness of siRNA in vivo, and the present technology might support the development of siRNA medicines.

## ACKNOWLEDGMENT

This study was financially supported by the Health and Labor Sciences Research Grants from the Ministry of Health, Labour, and Welfare of Japan. Synthesis of positron emitter-labeled siRNA was supported in part by Hokkaido System Science Co. Ltd. We thank Drs. T. Kakiuchi and H. Uchida at Hamamatsu Photonics K.K. PET Center for PET study for their technical assistance. They also thank Drs. S. Akai and T. Toyo'oka at the University Shizuoka for their valuable discussions as well as for allowing us to use their facilities. We also acknowledge Dr. S. Inagaki for helpful discussions and excellent technical assistance.

**Supporting Information Available:** Preparation of [ $^3\text{H}$ ]-labeled liposome and complex. Biodistribution of liposomes and complexes. This material is available free of charge via the Internet at <http://pubs.acs.org>.

## LITERATURE CITED

- (1) Fire, A., Xu, S., Montgomery, M. K., Kostas, S. A., Driver, S. E., and Mello, C. C. (1998) Potent and specific genetic interference by double-stranded RNA in *Caenorhabditis elegans*. *Nature* 391, 806–811.
- (2) Elbashir, S. M., Harborth, J., Lendeckel, W., Yalcin, A., Weber, K., and Tuschl, T. (2001) Duplexes of 21-nucleotide RNAs mediate RNA interference in cultured mammalian cells. *Nature* 411, 494–498.
- (3) Pai, S. I., Lin, Y. Y., Macaes, B., Meneshian, A., Hung, C. F., and Wu, T. C. (2006) Prospects of RNA interference therapy for cancer. *Gene Ther.* 13, 464–477.
- (4) Jeong, J. H., Mok, H., Oh, Y. K., and Park, T. G. (2009) siRNA conjugate delivery systems. *Bioconjugate Chem.* 20, 5–14.
- (5) Zimmermann, T. S., Lee, A. C. H., Akinc, A., Bramlage, B., Bumcrot, D., Fedoruk, M. N., Harborth, J., Heyes, J. A., Jeffs, L. B., John, M., Judge, A. D., Lam, K., McClintock, K., Nechev, L. V., Palmer, L. R., Racie, T., Rohl, I., Seiffert, S., Shanmugam, S., Sood, V., Soutschek, J., Toudjarska, I., Wheat, A. J., Yaworski, E., Zedalis, W., Kotliansky, V., Manoharan, M., Vormlocher, H. P., and MacLachlan, I. (2006) RNAi-mediated gene silencing in non-human primates. *Nature* 441, 111–114.
- (6) Kim, S. H., Jeong, J. H., Lee, S. H., Kim, S. W., and Park, T. G. (2008) LHRH receptor-mediated delivery of siRNA using polyelectrolyte complex micelles self-assembled from siRNA-PEG-LHRH conjugate and PEI. *Bioconjugate Chem.* 19, 2156–2162.
- (7) Medarova, Z., Pham, W., Farrar, C., Petkova, V., and Moore, A. (2007) In vivo imaging of siRNA delivery and silencing in tumors. *Nat. Med.* 13, 372–377.
- (8) Urakami, T., Akai, S., Katayama, Y., Harada, N., Tsukada, H., and Oku, N. (2007) Novel amphiphilic probes for [ $^{18}\text{F}$ ]-radiolabeling preformed liposomes and determination of liposomal trafficking by positron emission tomography. *J. Med. Chem.* 50, 6454–6457.
- (9) Bartlett, D. W., Su, H., Hildebrandt, I. J., Weber, W. A., and Davis, M. E. (2007) Impact of tumor-specific targeting on the biodistribution and efficacy of siRNA nanoparticles measured by multimodality in vivo imaging. *Proc. Natl. Acad. Sci. U.S.A.* 104, 15549–15554.
- (10) Viel, T., Kuhnast, B., Hinnen, F., Boisgard, R., Tavitian, B., and Dolle, F. (2007) Fluorine-18 labelling of small interfering RNAs (siRNAs) for PET imaging. *J. Labelled Compd. Radiopharm.* 50, 1159–1168.
- (11) Viel, T., Boisgard, R., Kuhnast, B., Jegou, B., Siquier-Pernet, K., Hinnen, F., Dolle, F., and Tavitian, B. (2008) Molecular imaging study on in vivo distribution and pharmacokinetics of modified small interfering RNAs (siRNAs). *Oligonucleotides* 18, 201–212.
- (12) Chen, X., Park, R., Shahinian, A. H., Tohme, M., Khankaldyyan, V., Bozorgzadeh, M. H., Bading, J. R., Moats, R., Laug, W. E., and Conti, P. S. (2004) 18F-labeled RGD peptide: initial evaluation for imaging brain tumor angiogenesis. *Nucl. Med. Biol.* 31, 179–189.
- (13) Vaidyanathan, G., and Zalutsky, M. R. (1994) Improved synthesis of N-succinimidyl 4-[ $^{18}\text{F}$ ]fluorobenzoate and its application to the labeling of a monoclonal-antibody fragment. *Bioconjugate Chem.* 5, 352–356.
- (14) Li, J., Trent, J. O., Bates, P. J., and Ng, C. K. (2006) Labeling G-rich oligonucleotides (GROs) with N-succinimidyl 4-[ $^{18}\text{F}$ ]fluorobenzoate (S18FB). *J. Labelled Compd. Radiopharm.* 49, 1213–1221.
- (15) Haka, M. S., Kilbourn, M. R., Watkins, G. L., and Toorongian, S. A. (1989) Aryltrimethylammonium trifluoromethanesulfonates as precursors to aryl [ $^{18}\text{F}$ ] fluorides: improved synthesis of [ $^{18}\text{F}$ ] GBR-13119. *J. Labelled Compd. Radiopharm.* 27, 823–833.
- (16) Harada, N., Ohba, H., Fukumoto, D., Kakiuchi, T., and Tsukada, H. (2004) Potential of [ $^{18}\text{F}$ ] $\beta$ -CFT-FE ( $\beta$ -carbomethoxy-3 $\beta$ -(4-fluorophenyl)-8-(2-[ $^{18}\text{F}$ ]fluoroethyl)nortropane) as a dopamine transporter ligand: A PET study in the conscious monkey brain. *Synapse* 54, 37–45.
- (17) Tang, G., Zeng, W. B., Yu, M. X., and Kabalka, G. (2008) Facile synthesis of N-succinimidyl 4-[ $^{18}\text{F}$ ]fluorobenzoate ([ $^{18}\text{F}$ ]SFB) for protein labeling. *J. Labelled Compd. Radiopharm.* 51, 68–71.
- (18) Takamatsu, H., Kakiuchi, T., Noda, A., Uchida, H., Nishiyama, S., Ichise, R., Iwashita, A., Mihara, K., Yamazaki, S., Matsuoka, N., Tsukada, H., and Nishimura, S. (2004) An application of a new planar positron imaging system (PPIS) in a small animal: MPTP-induced parkinsonism in mouse. *Ann. Nucl. Med.* 18, 427–431.
- (19) Uchida, H., Okamoto, T., Ohmura, T., Shimizu, K., Satoh, N., Koike, T., and Yamashita, T. (2004) A compact planar positron imaging system. *Nucl. Instrum. Methods Phys. Res., Sect. A* 516, 564–574.

- (20) Uchida, H., Sato, K., Kakiuchi, T., Fukumoto, D., and Tsukada, H. (2008) Feasibility study of quantitative radioactivity monitoring of tumor tissues inoculated into mice with a planar positron imaging system (PPIS). *Ann. Nucl. Med.* 22, 57–63.
- (21) de Fougerolles, A. R. (2008) Delivery vehicles for small interfering RNA *in vivo*. *Hum. Gene Ther.* 19, 125–32.
- (22) Bauer, M., Wagner, C. C., and Langer, O. (2008) Microdosing studies in humans: the role of positron emission tomography. *Drugs in R&D* 9, 73–81.
- (23) Wagner, C. C., Muller, M., Lappin, G., and Langer, O. (2008) Positron emission tomography for use in microdosing studies. *Curr. Opin. Drug Discovery Dev.* 11, 104–110.
- (24) Litzinger, D. C., Brown, J. M., Wala, I., Kaufman, S. A., Van, G. Y., Farrell, C. L., and Collins, D. (1996) Fate of cationic liposomes and their complex with oligonucleotide *in vivo*. *Biochim. Biophys. Acta, Biomembr.* 1281, 139–149.
- (25) Li, S., Tseng, W. C., Stolz, D. B., Wu, S. P., Watkins, S. C., and Huang, L. (1999) Dynamic changes in the characteristics of cationic lipidic vectors after exposure to mouse serum: implications for intravenous lipofection. *Gene Ther.* 6, 585–594.
- (26) McLean, J. W., Fox, E. A., Baluk, P., Bolton, P. B., Haskell, A., Pearlman, R., Thurston, G., Umemoto, E. Y., and McDonald, D. M. (1997) Organ-specific endothelial cell uptake of cationic liposome-DNA complexes in mice. *Am. J. Physiol.* 273, H387–404.
- (27) van de Water, F. M., Boerman, O. C., Wouterse, A. C., Peters, J. G., Russel, F. G., and Masereeuw, R. (2006) Intravenously administered short interfering RNA accumulates in the kidney and selectively suppresses gene function in renal proximal tubules. *Drug Metab. Dispos.* 34, 1393–1397.
- (28) Lendvai, G., Velikyan, I., Bergstrom, M., Estrada, S., Laryea, D., Valila, M., Salomaki, S., Langstrom, B., and Roivainen, A. (2005) Biodistribution of <sup>68</sup>Ga-labelled phosphodiester, phosphorothioate, and 2'-O-methyl phosphodiester oligonucleotides in normal rats. *Eur. J. Pharm. Sci.* 26, 26–38.
- (29) Braasch, D. A., Paroo, Z., Constantinescu, A., Ren, G., Oz, O. K., Mason, R. P., and Corey, D. R. (2004) Biodistribution of phosphodiester and phosphorothioate siRNA. *Bioorg. Med. Chem. Lett.* 14, 1139–1143.
- (30) Liu, N., Ding, H., Vanderheyden, J. L., Zhu, Z., and Zhang, Y. (2007) Radiolabeling small RNA with technetium-99m for visualizing cellular delivery and mouse biodistribution. *Nucl. Med. Biol.* 34, 399–404.

BC9005267